

Differentiation of Human Adipose-Derived Stem Cells into Fat Involves Reactive Oxygen Species and Forkhead Box O1 Mediated Upregulation of Antioxidant Enzymes

Masayoshi Higuchi,^{1,2} Gregory J. Dusting,¹⁻³ Hitesh Peshavariya,^{1,2} Fan Jiang,⁴
Sarah Tzu-Feng Hsiao,^{2,3} Elsa C. Chan,^{1,2} and Guei-Sheung Liu^{1,2}

Both reactive oxygen species (ROS) and Forkhead box O (FOXO) family transcription factors are involved in the regulation of adipogenic differentiation of preadipocytes and stem cells. While FOXO has a pivotal role in maintaining cellular redox homeostasis, the interactions between ROS and FOXO during adipogenesis are not clear. Here we examined how ROS and FOXO regulate adipogenesis in human adipose-derived stem cells (hASC). The identity of isolated cells was confirmed by their surface marker expression pattern typical for human mesenchymal stem cells (positive for CD29, CD44, CD73, CD90, and CD105, negative for CD45 and CD31). Using a standard adipogenic cocktail consisting of insulin, dexamethasone, indomethacin, and 3-Isobutyl-1-methylxanthine (IDII), adipogenesis was induced in hASC, which was accompanied by ROS generation. Scavenging ROS production with N-acetyl-L-cysteine or EUK-8, a catalytic mimetic of superoxide dismutase (SOD) and catalase, inhibited IDII-induced adipogenesis. We then mimicked IDII-induced oxidative stress through a lentiviral overexpression of Nox4 and an exogenous application of hydrogen peroxide in hASC and both manipulations significantly enhanced adipogenesis without changing the adipogenic differentiation rate. These data suggest that ROS promoted lipid accumulation in hASC undergoing adipogenesis. Antioxidant enzymes, including SOD2, catalase, and glutathione peroxidase were upregulated by IDII during adipogenesis, and these effects were blunted by FOXO1 silencing, which also suppressed significantly IDII-induced adipogenesis. Our findings demonstrated a balance of ROS generation and endogenous antioxidants in cells undergoing adipogenesis. Approaches targeting ROS and/or FOXO1 in adipocytes may bring new strategies to prevent and treat obesity and metabolic syndrome.

Introduction

OBESITY HAS BEEN RECOGNIZED as a major risk factor for the development of type 2 diabetes, heart disease, hypertension, and stroke [1,2] throughout the world, and is characterized by enlarged adipose tissues comprised of hypertrophied or hyperplastic adipocytes [3,4]. Adipocytes can be derived from pluripotent mesenchymal stem cells (MSCs) that have potentials to differentiate into various cell lineages [5]. Adipogenesis is thought to occur in 2 stages: commitment of MSC to a preadipocyte fate, and terminal differentiation to adipocytes [6]. Several studies have revealed that regulation of adipogenesis in the mouse preadipocyte line 3T3-L1 involves multiple pathways, including a sequential activation of transcription factors CCAAT/enhancer-binding proteins

(C/EBPs) and peroxisome proliferator-activated receptor γ (PPAR γ) and, ultimately, converge to cause an induction of metabolic genes associated with an adipocyte phenotype, such as adipocyte protein 2 (aP2), also known as fatty acid-binding protein 4 and glucose transporter 4 [6,7]. In contrast, little is known about how adipogenesis is regulated in human adipose-derived stem cells (hASC). Gimble et al. [8] recently isolated a population of MSC termed hASC from human fat and found them possessing multi-lineage differentiation potentials. These cells were differentiated to fat, bone, cartilage, vascular, and muscle lineages following directed differentiation [8].

Reactive oxygen species (ROS) are implicated in the modulation of cell functions, such as proliferation, differentiation, and survival [9,10]. Indeed intracellular ROS

¹Centre for Eye Research Australia, East Melbourne, Australia.

²O'Brien Institute, Fitzroy, Australia.

³Department of Surgery, University of Melbourne, Victoria, Australia.

⁴Key Laboratory of Cardiovascular Remodeling and Function Research, Chinese Ministry of Education and Chinese Ministry of Health, Qilu Hospital, Shandong University, Jinan, China.

generation has been found to regulate the enzymatic activity of target proteins via covalent modification [11–14]. ROS derived from nicotinamide adenine dinucleotide phosphate (NADPH) oxidase [15] and mitochondria [16] appear to have a role in adipogenic differentiation. It was demonstrated that the augmented ROS production accompanying adipogenesis in adipocyte was abolished by an NADPH oxidase inhibitor [15]. On the other hand, there is evidence that ROS derived from mitochondrial complex III may promote adipogenesis via an upregulation of C/EBP α and PPAR γ in human bone marrow MSC [16]. Indeed ROS have been found to facilitate the dimerization of C/EBP β , leading to an expression of a downstream adipogenic effector C/EBP α [17]. How ROS regulate adipogenesis in hASC remains unclear.

Recently, many reports have demonstrated that the forkhead box O transcription factors (FOXOs) are induced under oxidative stress [10,18] and are involved in the regulation of adipogenic differentiation [19,20]. FOXOs are the mammalian homolog of Daf-16 in nematodes, and the functions of FOXO proteins are tightly controlled by Akt-mediated phosphorylation [21,22]. FOXO members have highly conserved Akt phosphorylation sites. The phosphorylated FOXO proteins bind to 14-3-3 chaperone proteins, and are then sequestered in the cytoplasm, where they are unable to regulate gene expression [23,24]. Previous studies have suggested that FOXO members are involved in the regulation of adipogenesis, but their precise roles are still controversial [19,20]. For example, an overexpression of an activated form of FOXO1 in the mouse 3T3-F442A preadipocytes suppressed adipogenesis by inhibiting clonal expansion of the progenitor cells [19], while other authors demonstrated that silencing of FOXO1 impaired adipogenic differentiation in 3T3-L1 cells [20]. The effects of FOXO proteins in adipogenic differentiation of hASC, however, are not understood.

Cells undergoing adipogenesis are likely to upregulate antioxidant enzymes to avoid cellular damage or cell death caused by oxidative stress [25,26]. In this study, we investigated how ROS regulate the process of adipogenesis and how cells maintain the cellular redox homeostasis through FOXO1-mediated antioxidation systems during adipogenesis in hASC.

Materials and Methods

Reagents

Insulin, dexamethasone, indomethacin, isobutylmethylxanthine (IBMX), N-acetyl-L-cysteine (NAC), rotenone, diphenylethiodonium (DPI), allopurinol, 2',7'-dichlorofluorescein diacetate (DCFDA), penicillin, sodium thiosulfate, β -glycerophosphate, and silver nitrate were purchased from Sigma-Aldrich. EUK-8 and Hydrogen peroxide were purchased from Merck Millipore.

Isolation and culture of hASC

Human ASC isolation was performed as previously described with some modifications [27]. This procedure was approved by St Vincent's Hospital Human Ethics Committee (HREC5203). Human fat tissues were excised from patients undergoing plastic surgery. Excised tissues were washed using phosphate-buffered saline (PBS) supplemented with

antibiotics (100 mg/mL streptomycin and 100 U/mL penicillin; Invitrogen, Carlsbad, CA), and then minced into pieces of ~ 1 mm³. Minced fat tissues were mixed with PBS and centrifuged at 1000 rpm for 8 min. The floating fat layer was collected and digested in 3 \times volume of the high-glucose Dulbecco's modified Eagle's medium (DMEM; Invitrogen) supplemented with 0.5 mg/mL collagenase I (250 U/mg; Worthington) and antibiotics, with continuous shaking overnight at 37°C. On the second day, isolated cells were collected by centrifugation (1200 rpm, 10 min), resuspended in PBS, and passed through a cell strainer. After 2 additional centrifugations, cells were seeded in culture flasks and cultured overnight at 37°C with 5% CO₂ in the high-glucose DMEM supplemented with 10% fetal bovine serum (FBS, from PAA) and antibiotics. On the third day, attached cells were rinsed 3 times with PBS to remove red blood cells and further cultured in the keratinocyte complete medium (keratinocyte-SFM from Invitrogen) supplemented with 5% FBS, 50 μ g/mL bovine pituitary extract, and 5 ng/mL recombinant epidermal growth factor. The keratinocyte medium was used because there was evidence that this medium could enhance proliferation, while maintaining stemness of hASC. Confluent cells were subcultured by trypsinization at a 1:4 ratio.

Characterization of hASC

1×10^5 hASC were resuspended in 50 μ L of 2.5% fetal calf serum (FCS) in PBS and incubated with fluorescent-conjugated antibodies against CD31 (platelet/endothelial cell adhesion molecule; 1:50 dilutions), CD45 (leukocyte common antigen; 1:50 dilutions), CD29 (β 1-integrin; 1:50 dilutions), CD44 (gp85; 1:50 dilutions), CD73 (5'-nucleotidase; 1:100 dilutions), CD90 (Thy-1; 1:200 dilutions), or CD105 (endoglin; 1:100 dilutions) (BD Biosciences) on ice for 30 min with light shielding. Control cells were incubated with the appropriate isotype control antibodies (BD Biosciences). Flow cytometry analysis was performed using a FACSCanto II (BD Biosciences). Cells were gated to exclude cell debris and 1×10^4 events were acquired and analyzed using BD FACSDiva Software v6.0 (BD Biosciences). The surface marker expression pattern typical for human MSCs was CD29-, CD44-, CD73-, CD90-, and CD105-positive; CD45- and CD31-negative.

Adipogenic differentiation of hASC

To determine adipogenic differentiation ability of hASC, confluent cells were continuously cultured in the adipogenic medium for 8 days. The medium contained: the Minimum Essential Medium (Invitrogen) supplemented with 10% FCS, 1% antibiotic/antimycotic, 0.5 mM IBMX, 10 μ M insulin, 1 μ M dexamethasone, and 0.2 mM indomethacin. The adipogenic medium was changed every second day. Oil red O staining was used to assess the accumulation of intracellular lipid droplets.

Determination of lipid accumulation with Oil red O assay

Cells were fixed with 10% neutral-buffered formalin for 40 min at room temperature. After fixation, cells were rinsed in 3 changes of PBS for 10 min, and then distilled water. Oil

red O stock (0.5% in 98% isopropyl alcohol; BDH Chemicals) was diluted with distilled water (volume ratio=3: 2) and filtered. Cells were incubated for 50 min to stain intracellular lipid droplets, and counterstained with Mayer's Hematoxylin. To evaluate the degree of adipogenic differentiation, 5 random photos were taken under 400 \times microscope and cells carrying red lipid droplets were counted as differentiated. The adipogenic differentiation rate was calculated as the ratio of the adipocyte number to the total cell number in each image.

AdipoRed assay

Intracellular lipid accumulation was quantified using the AdipoRed Adipogenesis Assay Reagent (Lonza, Basel, Switzerland) according to the manufacturer's protocol. Briefly, cells were prewashed with PBS once and incubated with the AdipoRed Reagent for 10 min. Trypsinized cells were analyzed by FACSCanto II (BD Biosciences) or subject to fluorescence assay at excitation 485 nm and emission 572 nm, using a Polarstar microplate reader (BMG Labtech) at 37°C.

ROS measurement

The intracellular ROS level was assessed using DCFDA as previously described [28]. Cells were plated at a seeding density of 1×10^4 cells/cm² in 12- or 96-well plates and subjected to adipogenic differentiation. On day 8, cells were washed with the Hanks balanced salt solution, loaded with 10 μ M DCFDA, and incubated for 30 min at 37°C. The fluorescence intensity of 2',7'-dichlorofluorescein was measured using a FACSCanto II or Polarstar microplate reader at excitation 480 nm and emission 530 nm.

Amplex Red assay

Extracellular H₂O₂ was detected using Amplex® Red assay as previously described [28]. Cells seeded at 1×10^4 cells/cm² in 96-well plates were subject to adipogenic differentiation. On day 0, 2, and 8, cells were harvested by trypsinization and incubated in the Krebs-HEPES buffer (98 mM NaCl, 4.7 mM KCl, 25 mM NaHCO₃, 1.2 mM MgSO₄, 1.2 mM KH₂PO₄, 2.5 mM CaCl₂, 11.1 mM D-glucose, and 20 mM Hepes-Na) containing the Amplex® Red reagent (Invitrogen). Fluorescence was then measured at excitation 571 nm and emission 585 nm using the Polarstar microplate reader at 37°C.

Quantitative real-time PCR

The quantitative polymerase chain reaction (PCR) was performed to verify the expression of human genes, including FOXOs, C/EBP α , PPAR γ , aP2, superoxide dismutase (SOD)1, SOD2, catalase, and glutathione peroxidase (GPx)1/2. Total RNA from treated cells was extracted with the Trizol reagent (Ambion) according to the manufacturer's instructions and reverse-transcribed to cDNA using the High-capacity cDNA reverse transcription kit (Applied Biosystems) at 25°C for 10 min, 37°C for 2 h, and 70°C for 10 min in a thermal cycler (BioRad-DNA Engine). The real-time PCR reactions were performed in a 7300 system (Applied Biosystems) using TaqMan Universal PCR master mix and

predesigned gene-specific probes and primer sets for human catalase (Hs00156308_m1), SOD1 (Hs00916176_m1), SOD2 (Hs01553554_m1), GPx1 (Hs02516751_s1), FOXO1 (Hs01054576_m1), FOXO3 (Hs00921424_m1), FOXO4 (Hs00172973_m1), and GAPDH (huGAPDH 4326317E)) or using SYBR green universal PCR Master mix (Applied Biosystems, VIC, Australia) and primers for PPAR γ , C/EBP α , aP2, and GAPDH as described in Supplementary Materials and Methods. Data were normalized to GAPDH (4326317E) and expressed as fold changes over that in the control treatment group.

Lentiviral-based expression of Nox4 NADPH oxidase

The packaging system for lentiviral production, including vectors pCMV- Δ R8.91, pMD.G (envelope element), and pLKO_AS2/Nox4.puro (transfer vector) were obtained from the National RNAi Core Facility (Taiwan). Briefly, 6×10^5 HEK293T cells were seeded in a 6-cm culture dish and cultured for 24 h. A mixture of the 3 vectors (2.3 μ g pCMV- Δ R8.91, 0.3 μ g pMD.G, and 2.5 μ g transfer vector) was prepared and transfected into 293T cells using Lipofectamine 2000 (Invitrogen). The virus-containing medium was collected at 48 h after transfection. For lentiviral transduction, 1×10^5 hASC were seeded in 6-well plates in a medium containing 8 μ g/mL polybrene (Sigma-Aldrich). The culture medium was removed at 24 h postinfection and replaced with a medium containing 1 μ g/mL puromycin (Sigma-Aldrich). Successfully transduced cells were identified as those growing in the presence of puromycin (1 μ g/mL) for 7 days.

Western blot

The protein extract was isolated from cells using the lysis buffer containing 150 mM NaCl, 50 mM HEPES pH 7, 1% Triton X-100, 10% glycerol, 1.5 mM MgCl₂, 1 mM EGTA, and protease inhibitors (Roche Applied Science). After separation in 12.5% sodium dodecyl sulfate-polyacrylamide gel electrophoresis, the protein was transferred onto a polyvinylidene fluoride membrane using a blotting apparatus. The membrane was blocked with 5% skim milk in TBS-T for 1 h at room temperature, and then incubated with one of the following antibodies for FOXO1A (rabbit polyclonal, 1:500 dilutions; Abcam), FOXO3A (rabbit polyclonal, 1:500 dilutions; Abcam), catalase (mouse monoclonal, 1:500 dilutions; Sigma-Aldrich), SOD1 (sheep polyclonal, 1:1000 dilutions; BD Biosciences), SOD2 (sheep polyclonal, 1:1000 dilutions; BD Biosciences), or GPx-1/2 (mouse monoclonal, 1:500 dilutions; Santa Cruz Biotechnology) overnight at 4°C or β -actin (mouse monoclonal, 1:2000 dilutions; Millipore) for 30 min at room temperature. After incubation with the secondary antibody conjugated with horseradish peroxidase (1:5000 dilutions in 5% skim milk) for 30 min, the signals on the membrane were detected using the ECL-plus luminol solution (Pharmacia) and exposed to X-ray film for autoradiogram.

RNA Interference

To knockdown gene expression, ON-TARGETplus™ for nontargeting control, human FOXO1 and FOXO3 siRNAs were purchased from Thermo Scientific (Supplementary

Materials and Methods). Cells were transfected with siRNAs using the DharmaFECT 1 reagent (Thermo Scientific) according to the manufacturer's instruction. Briefly, cells were seeded in 6- or 12-well plates in the medium containing serum 24 h before transfection. Cells were transfected with 100 nM siRNA and DharmaFECT 1 reagent for 48 h. The siRNA targeting sequence for human FOXO1 and human FOXO3 is described in Supplementary Materials and Methods.

Data and statistics

All values are presented as mean \pm standard error of the mean. Statistical analysis was carried out using one-way analysis of variance followed by the Newman-Keuls t-test (for multiple comparisons) unless indicated otherwise. A *P*-value less than 0.05 was regarded as statistically significant.

Results

Characterization of human ASC and adipogenic differentiation

Human ASC were successfully isolated from human abdominal fat flaps and both serpiginous and fibroblast-like cells were observed in primary cultures, consistent with previous descriptions of hASC [27]. Undifferentiated cells were characterized using flow cytometry with surface markers for hASC [29]. As shown in Supplementary Fig. S1 (Supplementary Data are available online at www.liebertpub.com/scd), the majority of isolated cells were positive for stem cell markers CD29, CD44, CD73, CD90, and CD105, while less than 0.1% of the cells were positive for the hematopoietic marker CD45 and the endothelial cell marker CD31 (Supplementary Fig. S1A) [30]. Furthermore, hASC demonstrated *in vitro* ability to differentiate into adipogenic, osteogenic, and chondrogenic lineages (Supplementary Fig. S1B). These experiments confirmed that the isolated hASC possessed stem cell properties.

The adipogenic cocktail consisting of insulin, dexamethasone, indomethacin, and IBMX (IDII) has been used to induce adipogenesis of hASC [5]. Here we demonstrated that IDII treatment induced hASC differentiation into adipocytes, as evidenced by the expression of adipogenesis markers C/EBP α , PPAR γ , and aP2, in a time-dependent manner (6–8 days) (Supplementary Fig. S2A). Next, we analyzed the extent of lipid accumulation as an indicator of adipogenesis. As shown in Supplementary Fig. S2B, hASC treated with IDII showed a significant increase in intracellular lipid accumulation as revealed by Oil red O staining (the percentages of differentiation on day 8 in control and IDII-treated hASC were $4.2\% \pm 1.5\%$ and $35.3\% \pm 1.9\%$, respectively; $P < 0.01$). We also validated our findings with a conventional AdipoRed assay to quantify cellular triglyceride contents. There was a marked increase in intracellular triglyceride droplets in IDII differentiated cells (Supplementary Fig. S2C).

ROS are involved in promoting adipocyte lineage differentiation of human ASC

There is evidence that ROS generation regulates adipogenic differentiation in human bone marrow-derived MSC and the mouse 10T1/2 cell line [16,31]. To investigate whe-

ther IDII-induced adipogenic differentiation was dependent on ROS in hASC, we measured intracellular and extracellular ROS generation with DCFDA and Amplex Red assays, respectively. As shown in Fig. 1A, IDII treatment stimulated intracellular ROS generation, which was mainly localized in differentiated cells. Furthermore, quantification of the DCFDA fluorescent intensity by flow cytometry revealed an increase in DCFDA signals in differentiated cells. Amplex Red assay also confirmed the elevated ROS generation in IDII-differentiated hASC on day 8 (Fig. 1B). To explore the role of ROS in IDII-induced hASC differentiation, we treated cells with NAC, an antioxidant compound and EUK-8, a catalase and SOD mimetic, throughout the induction to abolish the stimulatory effect of IDII on ROS production as detected by Amplex red (Fig. 1C). We next demonstrated that both NAC and EUK-8 partially, but significantly suppressed IDII-induced adipogenic differentiation (reduced proportion of differentiated cell number by Oil red O staining and expression of the adipocyte marker, aP2; Fig. 1D, E).

Intriguingly, in the Oil red O stained cells, the lipid droplets in differentiated cells (insert of Fig. 1F) were shrunk by antioxidants treatment, suggesting that reduced ROS may suppress not only adipogenic differentiation, but also lipid accumulation in differentiated cells. To further confirm the effects of ROS on lipid accumulation in differentiated hASC, we measured the accumulation of intracellular triglyceride droplets detected by AdipoRed assay. It was found that the lipid droplets in differentiated cells were significantly reduced in NAC-treated cells (Fig. 1G). We then used flow cytometry to sort the cells stained with AdipoRed and identified 3 populations: undifferentiated, low-density lipid accumulation, and high-density lipid accumulation in the cells. As illustrated by the scatter plot and quantitative bar graph in Fig. 1H, NAC treatment significantly reduced the number of both high density and low density of lipid accumulation in cells. Taken together, these findings indicate that IDII-induced adipogenesis is dependent on ROS production in hASC.

Moreover, we characterized the source of ROS generation during IDII-induced adipogenesis using inhibitors to antagonize the contribution of different enzymes in the late stage of hASC differentiation (day 8): rotenone (mitochondrial electron transport chain), DPI (NADPH oxidases), and allopurinol (xanthine oxidoreductase) and then measured ROS production by DCFDA assay. Although ROS generation was inhibited by all 3 inhibitors (see Table 1), the degree of IDII-induced accumulation of triglyceride was suppressed by rotenone and DPI, but not allopurinol, suggesting that mitochondria [16] and NADPH oxidase [31], but not xanthine oxidase [32] are the major sources of ROS generation.

Mimicking oxidative stress by exogenous application of hydrogen peroxide and manipulation of ectopic Nox4 expression promotes adipogenesis

To further investigate whether ROS affected adipocyte differentiation in hASC, H₂O₂ (100 μ M) was incubated for 8 days during the standard differentiation procedure to mimic oxidative stress. As shown in Fig. 2, H₂O₂ treatment caused enhanced adipogenesis, as detected by Oil red O staining (Fig. 2A) and AdipoRed assay (Fig. 2B).

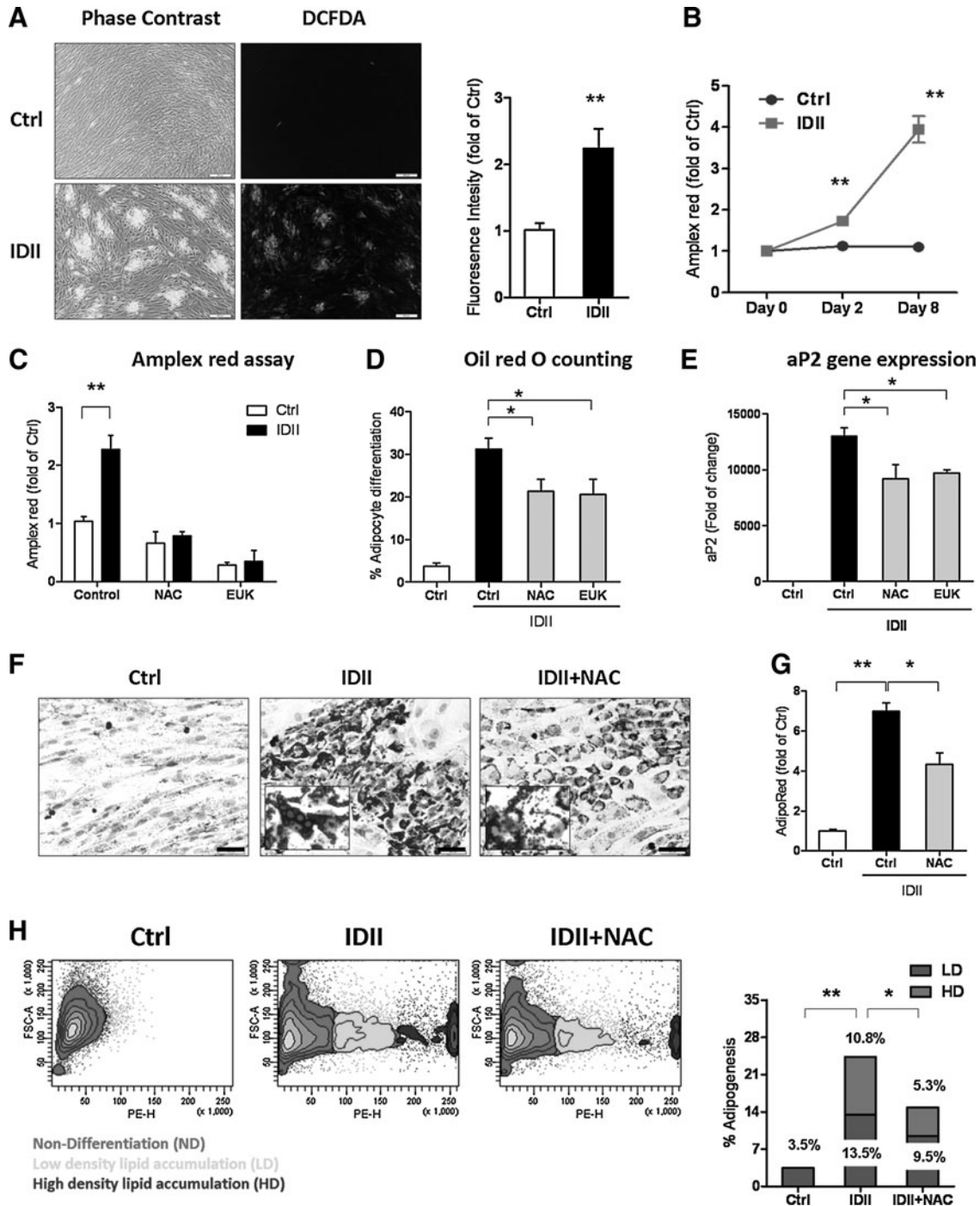


FIG. 1. Effects of reactive oxygen species (ROS) on differentiation of human adipose-derived stem cell (hASC) to adipocytes. **(A)** 2',7'-dichlorofluorescein diacetate (DCFDA) fluorescent images and quantification of fluorescent intensity showing localization of intracellular ROS generation concentrating in differentiated cells. **(B)** Extracellular ROS generation detected following 8 days of IDII induction by Amplex Red assay. **(C-H)** Cells were incubated with N-acetyl-L-cysteine (NAC) (10 mM) or EUK-8 (5 mM) throughout 8 days induction of adipogenic differentiation. The effect of NAC and EUK-8 on extracellular ROS generation was determined by Amplex red assay **(C)**, adipogenic differentiation by Oil red O counting **(D)** and adipocyte protein 2 (aP2) expression detected by real-time PCR **(E)**. The effect of NAC on lipid accumulation was determined by Oil red O staining **(F)**, AdipoRed assay **(G)**; intracellular triglyceride accumulation) and AdipoRed scatter plots **(H)**. The distribution of lipid droplets was characterized as high density (HD) and low density (LD) of undifferentiated (Ctrl) and IDII-differentiated hASC with and without NAC treatment. The insert shows a higher magnification (40 \times) of Oil red O-stained lipid droplets. Data are presented as mean \pm standard error of the mean (SEM) from 4 experiments. * $P < 0.05$ or ** $P < 0.01$ compared to control (ctrl). Scale bar represents 50 μ m.

TABLE 1. THE EFFECT OF ROTENONE, DPI, AND ALLOPURINOL ON ROS REDUCTION AFTER IDII INDUCTION IN hASC

	% of ROS reduction
IDII	0 ± 1.3
IDII + rotenone	40.5 ± 2.2 ^a
IDII + DPI	27.4 ± 9.9 ^a
IDII + allopurinol	15.9 ± 1.1 ^a

After 8 days of adipogenic induction, hASC were treated with rotenone (0.5 μM), DPI (0.1 μM), or allopurinol (50 μM) for 1 h and ROS generation from hASC was measured using DCFDA assay. ROS production was expressed as reduction from control groups. All data are presented as mean ± SEM from 3 to 4 experiments.

^a*P* < 0.05 compared with IDII alone.

hASC, human adipose-derived stem cell; DPI, diphenyleneiodonium; ROS, reactive oxygen species; DCFDA, 2',7'-dichlorofluorescein diacetate; SEM, standard error of the mean.

Nox4-derived ROS production has recently been implicated in the differentiation of adipocytes from rat bone marrow-derived MSC and human preadipocytes [31,33]. To confirm the involvement of ROS in adipogenic differentiation, we boosted ROS production by Nox4 overexpression to mimic the effect of IDII-induced ROS on adipogenesis. As compared to lenti-green fluorescent protein controls, lenti-Nox4 induced a remarkable increase in Nox4 expression and a 3-fold elevation of ROS generation (Fig. 3A). We then compared the effects of IDII treatment and lenti-Nox4 transduction in hASC on days 0, 2, and 8. As shown in Fig. 3B, lenti-Nox4 elevated ROS production to a level similar to that induced by IDII. Intriguingly, IDII did not further augment ROS production in lenti-Nox4-transfected cells. Moreover, we found that Nox4 overexpression enhanced adipogenesis and potentiated the accumulation of intracellular lipid in the presence or absence of IDII (Fig. 3C) in Day 8.

Upregulation of antioxidant enzymes during adipogenesis

Because we found that lentivirus-mediated Nox4 overexpression did not potentiate ROS generation in IDII-induced differentiated hASC, we explored the involvement of cellular antioxidant enzymes. Kojima et al. recently demonstrated that the expression of endogenous antioxidants, including catalase, SOD, and GPx were increased during

adipogenesis from 3T3 fibroblasts [25]. Therefore, we evaluated the expression of these enzymes in control and IDII-treated hASC. Similar to the results obtained in 3T3 fibroblasts, we found that IDII-induced hASC differentiation to adipocytes was accompanied by significant upregulation of SOD2, catalase, and the GPx gene as well as the protein level, whereas SOD1 was unaffected (Fig. 4A, B).

IDII-induced adipogenesis involves FOXO1

To delineate the mechanisms underlying ROS-dependent activation of antioxidant enzymes during adipogenesis, we explored the involvement of FOXO, a key transcriptional regulator in redox signaling [34]. To investigate whether FOXO proteins are involved in IDII-induced adipogenic differentiation, we performed real-time PCR analysis. We found that both FOXO1 and FOXO3, but not FOXO4, are abundantly expressed in hASC (Fig. 5A). In addition, FOXO1 and FOXO3 expression were significantly elevated during IDII-induced differentiation from day 1 (Fig. 5B). The upregulation of FOXO1 and FOXO3 in differentiated hASC was confirmed with western blot (Fig. 5C).

To further establish the effects of FOXOs modulating expression of antioxidant enzymes and adipogenesis, we silenced FOXO1 and FOXO3 gene expression by specific siRNAs. The efficiency and specificity of siRNA-mediated gene silencing was confirmed by PCR and western blot (Fig. 6A, B). Treatment with FOXO1 siRNA, but not FOXO3 siRNA, significantly inhibited upregulation of SOD2, catalase, and GPx1 during IDII-induced adipogenesis (Fig. 6C), indicating that FOXO1 mediated the upregulation of these antioxidant enzymes. Moreover, treatment with FOXO1 siRNA, but not FOXO3 siRNA, partially, yet significantly, suppressed IDII-induced aP2 expression and adipogenesis (Fig. 6D, E). These data suggest that FOXO1 has a pivotal role in regulation of antioxidant enzymes and adipogenesis in IDII-treated cells. In addition, we found that dexamethasone, but not other components in the IDII cocktail, was responsible for FOXO induction during adipogenesis (Supplementary Fig. S3).

Discussion

In this study, we demonstrated a novel role of ROS in promoting differentiation of hASC to the adipocyte lineage and a role of FOXO1 in maintaining cellular redox

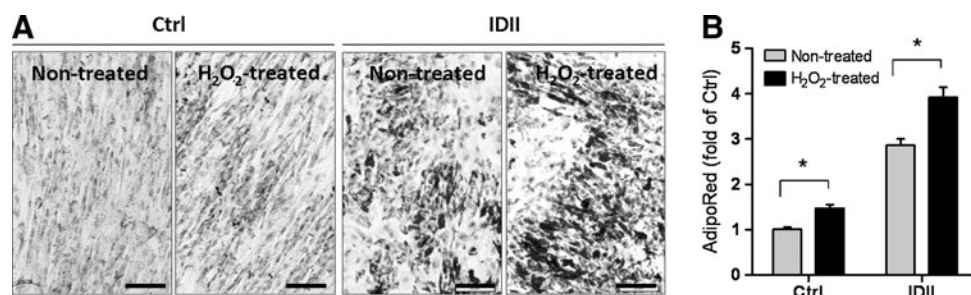


FIG. 2. Effects of hydrogen peroxide on adipogenic differentiation in hASC. hASC were incubated with hydrogen peroxide (H₂O₂; 100 μM) for 8 days with or without IDII induction, and adipogenesis was measured by Oil red O staining (A) and AdipoRed assay (B). Data are presented as mean ± SEM from 3 experiments. **P* < 0.05 compared to H₂O₂ treatment. Ctrl: control media; IDII: adipogenic differentiation media. Scale bar represents 50 μm.

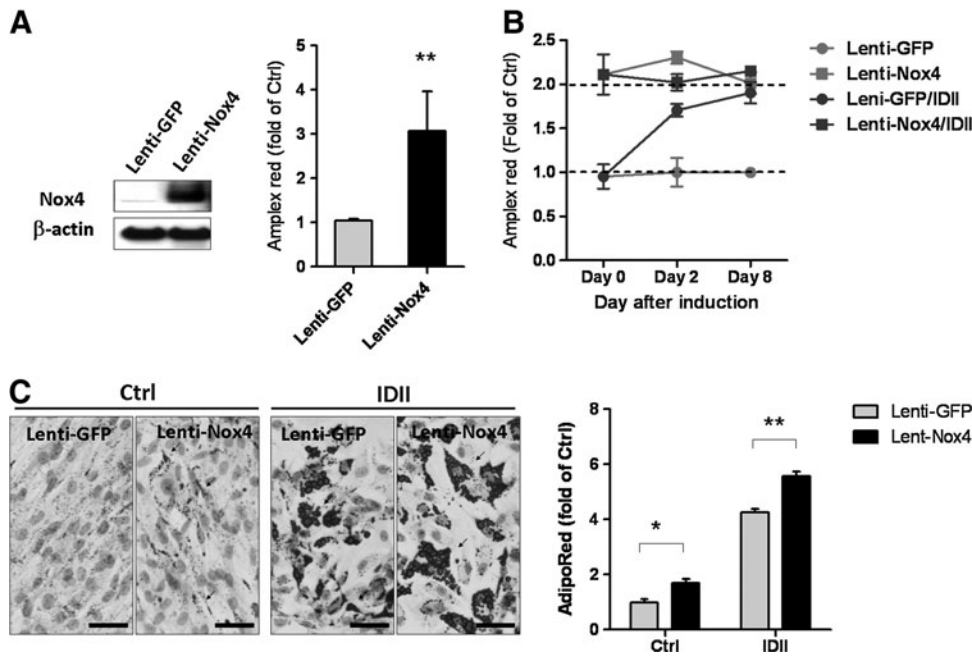
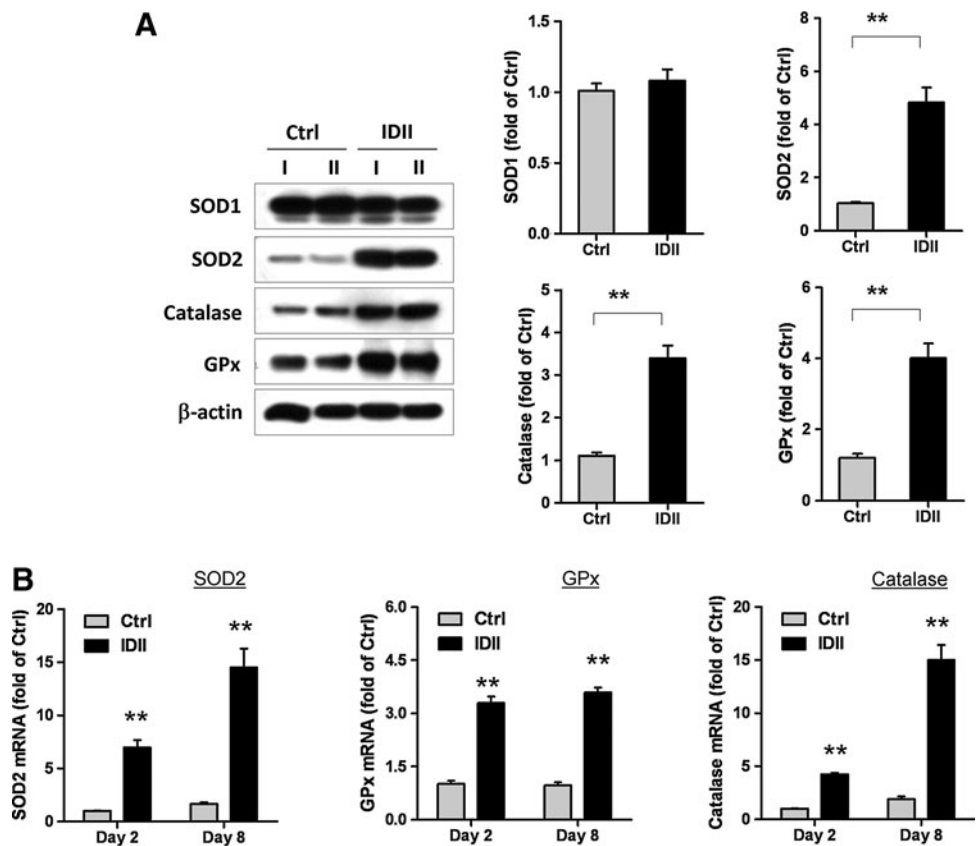


FIG. 3. Effects of ectopic Nox4 overexpression on ROS production and adipogenic differentiation in hASC. **(A)** Overexpression of Nox4 protein was detected in hASC transfected with a lentivirus carrying Nox4 (lenti-Nox4), but not in control lenti-green fluorescent protein (GFP) transfected cells. ROS generation detected by Amplex Red was increased by lenti-Nox4 transfection. **(B)** Effects of lenti-GFP and lenti-Nox4 transfected on ROS generation following 8 days with or without IDII induction, and determined by Amplex Red. **(C)** Effects of Nox4 overexpressing on adipogenic differentiation for 8 days with or without IDII induction, and adipogenesis was measured by Oil red O staining and AdipoRed assay in hASC. *Arrows* shown in representative photos indicate hASC differentiated into adipocytes. Data are presented as mean \pm SEM from 3 experiments. * $P < 0.05$ or ** $P < 0.01$ compared to lenti-GFP. Ctrl: control media; IDII: adipogenic differentiation media. Scale bar represents 20 μ m. *Arrow* indicates lipid drops.

FIG. 4. Expression of antioxidant enzymes during adipogenic differentiation in hASC. **(A)** Western blots and quantitative measures of protein expression of antioxidant enzymes superoxide dismutase (SOD)1, SOD2, catalase, and glutathione peroxidase (GPx) in undifferentiated and IDII-induced differentiated hASC on day 8. Two lineages of hASC from 2 different patients (I and II) were examined for western blot and representative data is shown. **(B)** The gene expression of SOD2, catalase, and GPx in hASC were examined by real-time PCR analysis on day 2 and day 8 following IDII treatment. Data are presented as mean \pm SEM from 6 experiments. ** $P < 0.01$ compared to control (Ctrl).



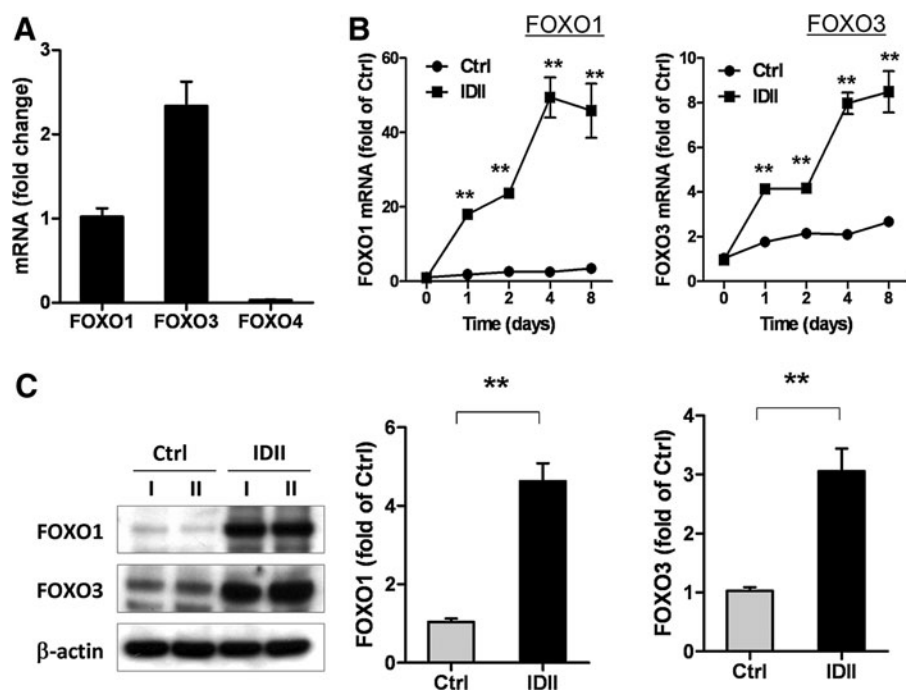


FIG. 5. Expression of forkhead box O (FOXO) transcription factors during adipogenic differentiation in hASC. The gene expression of FOXO1, FOXO3, and FOXO4 in undifferentiated hASC (A) and in differentiated hASC following 8 days of IDII induction (B) was examined by real-time PCR analysis. (C) The protein levels of FOXO1 and FOXO3 was measured by western blot, and level of protein was quantized by densitometry in undifferentiated (Ctrl) and IDII-differentiated hASC on day 8. Two lineages of hASC from 2 different patients (I and II) were examined for proteins and representative western blots are shown. Data are presented as mean \pm SEM from 6 experiments. ** $P < 0.01$ compared to control (Ctrl).

homeostasis during adipogenic differentiation. Using a cocktail of insulin, dexamethasone, indomethacin, and IBMX, we showed that induced adipogenic differentiation of hASC was accompanied by increased cellular ROS production, a response that was partially inhibited by the antioxidant agent NAC. Pretreatment with ROS scavengers decreased the proportion of cells exhibiting an adipocyte phenotype, and reduced the intracellular lipid content, suggesting that ROS promoted adipogenesis via 2 mechanisms: (1) inducing adipogenic differentiation and (2) encouraging intracellular lipid accumulation. Moreover, we found that NADPH oxidase and mitochondria are 2 major sources of ROS generation involved in these processes. Another finding in our study was that FOXO1, a key transcriptional regulator in redox signaling, is involved in regulating expression of endogenous antioxidant enzymes, such as SOD2, catalase, and GPx, during adipogenesis. This mechanism may protect cells from oxidative stress-induced damage during adipogenesis.

Several recent studies showed that ROS could regulate stem cell differentiation into adipocyte lineage, but the underlying signaling mechanisms remain unclear. Kanda et al. and Tormos et al. both showed that ROS generation was increased during adipogenesis in mouse MSC and human bone marrow-derived stem cells [16,31]. Similarly, we showed that differentiation of hASC to adipocytes was inhibited by ROS scavengers, confirming that ROS promote adipogenesis. We found that ROS not only induced ASC differentiation, but importantly, it also augmented accumulation of lipid droplets in differentiated cells, which is deeply involved in the pathogenesis of obesity. Intracellular lipid synthesis is facilitated by insulin signaling, which activates the Akt-mTORC1 pathway and thereby enhances expression of lipogenic enzymes through transcription factors SREBP-1 and PPAR γ [35]. ROS may augment insulin-triggered Akt signaling by inhibiting phosphatase and tensin homolog (PTEN), which has an oxidation-

sensitive cysteine residue in its catalytic active site [12]. In addition, there is evidence that ROS may facilitate dimerization of C/EBP β , leading to increased DNA binding activity of C/EBP β , which is required for terminal differentiation of adipocytes [17]. Our results also correlate with clinical data showing that there is a positive correlation between systemic oxidative stress and obesity [15,36]. Currently, hormonal regulation of adipogenesis is under intensive investigation, while the effects of oxidative stress on adipogenesis begin to gain some attention. Our results provided evidence that oxidative stress may be closely involved in regulating differentiation and maturation of adipogenic precursor cells, suggesting that targeting ROS may have a beneficial effect on obesity by preventing adipogenesis. Overexpressing Nox4 in ASC cells constantly generates ROS without any stimulation, which is comparable to the ROS level induced by IDII at early stages (day 0 and 2). However, we were unable to further potentiate ROS generation by IDII treatment in cells overexpressing Nox4, suggesting that an endogenous feedback mechanism might be activated by Nox4-dependent ROS generation, which limited further ROS generation.

Indeed, we observed that the expressions of SOD2, catalase, and GPx were remarkably increased during IDII-induced differentiation in hASC, and treatment with FOXO1 siRNA significantly inhibited the upregulation of these antioxidant enzymes. These are consistent with the notion that FOXO transcription factors have a pivotal role in maintaining the intracellular redox balance by regulating the expression of a variety of antioxidant enzymes [18,37]. However, it remains to be elucidated whether FOXO1-mediated expression of endogenous antioxidant enzymes act as a self-regulatory mechanism that has a feed-back effect on IDII-induced adipogenic differentiation. Nevertheless, our data support the notion that FOXO1 has an important role in maintaining intracellular redox homeostasis and preventing excessive oxidative stress during differentiation of stem cells [38].

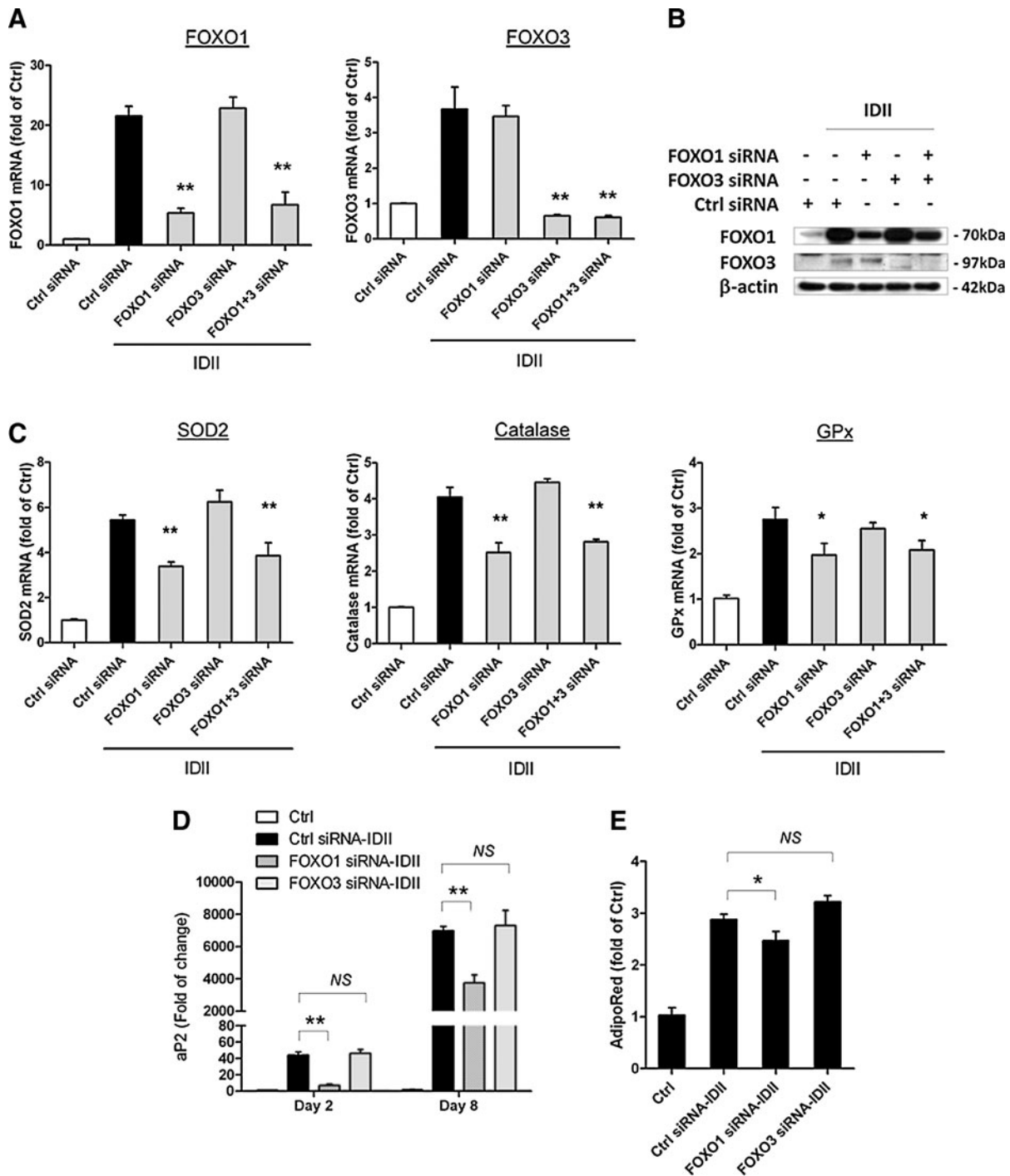


FIG. 6. Effects of FOXO gene silencing on expression of ROS antioxidant enzymes and adipogenesis in hASC. Effects of FOXO1 and FOXO3 siRNA on gene expression (**A**) and protein levels (**B**) of FOXO1 and FOXO3 were examined by western blot and real-time PCR analysis on day 8 after IDII induction. (**C**) Effects of FOXO1 and FOXO3 siRNA on gene expression of SOD2, catalase, and GPx in hASC were examined by real-time PCR analysis on day 8 after IDII induction. Effects of FOXO1 and FOXO3 siRNA on adipogenesis measured by gene expression of aP2 (**D**) and intracellular triglyceride accumulation detected with AdipoRed assay (**E**). Data are presented as mean \pm SEM from 6 experiments. * $P < 0.05$ or ** $P < 0.01$ compared to control (Ctrl) or siRNA control.

FOXO1 expression in hASC was upregulated after IDII treatment, and knockdown of FOXO1 partially inhibited IDII-induced adipogenesis. These data are consistent with those reported by Munekata and Sakamoto in 3T3-L1 pre-adipocytes, suggesting that FOXO1 has a positive role in

regulating adipogenic differentiation [20]. We further demonstrated that dexamethasone present in the IDII cocktail was responsible for FOXO1 upregulation (Supplementary Fig. S2), and this observation was in line with a recent report that glucocorticoids stimulated expression of FOXO family

transcription factors and increased insulin sensitivity in human primary preadipocytes [39]. In contrast, in mouse preadipocytes, it has been shown that overexpression of active FOXO1 repressed insulin-induced adipogenesis [19]. Moreover, it was demonstrated that FOXO1 was induced in the early stages of adipogenic differentiation of mouse 3T3-F442A preadipocytes, whereas FOXO activation was delayed until the end of the clonal expansion phase [19]. All these results suggest that regulation of FOXO expression and FOXO-mediated cellular responses during adipogenic differentiation are cell type- and context-dependent.

In conclusion, our data suggest that ROS may accelerate adipogenesis in hASC by enhancing differentiation and lipid accumulation, both of which are largely dependent on insulin signaling. Moreover, we suggest that FOXO1 may be a regulator of redox homeostasis during hASC differentiation, which limits excessive oxidative stress by upregulating antioxidant enzymes in hASC. Approaches targeting ROS and/or FOXO1 may bring new strategies for prevention or treatment of obesity.

Acknowledgments

This work was supported by project grants from the National Health and Medical Research Council of Australia (NHMRC 09007G) (G.L.), the JO&JR Wicking Trust, and the National Natural Science Foundation of China (NSFC81070164) (F.J.). G.J.D. is supported by a principal research fellowship from NHMRC. Centre for Eye Research Australia and O'Brien Institute acknowledges the Victorian State Government's Department of Innovation, Industry and Regional Development's Operational Infrastructure Support Program.

Author Disclosure Statement

The authors who have taken part in this study declared that they do not have anything to disclose regarding funding from industry or conflict of interest with respect to this manuscript.

References

- Rexrode KM, JE Manson and CH Hennekens. (1996). Obesity and cardiovascular disease. *Curr Opin Cardiol* 11:490–495.
- Ärnlöv J, E Ingelsson, J Sundström and L Lind. (2010). Impact of body mass index and the metabolic syndrome on the risk of cardiovascular disease and death in middle-aged men. *Circulation* 121:230–236.
- Spiegelman BM and JS Flier. (2001). Obesity and the regulation review of energy balance. *Cell* 104:531–543.
- Gesta S, YH Tseng and CR Kahn. (2007). Developmental origin of fat: tracking obesity to its source. *Cell* 131:242–256.
- Pittenger MF, AM Mackay, SC Beck, RK Jaiswal, R Douglas, JD Mosca, MA Moorman, DW Simonetti, S Craig and DR Marshak. (1999). Multilineage potential of adult human mesenchymal stem cells. *Science* 284:143.
- Cristancho AG and MA Lazar. (2011). Forming functional fat: a growing understanding of adipocyte differentiation. *Nat Rev Mol Cell Biol* 12:722–734.
- Farmer SR. (2006). Transcriptional control of adipocyte formation. *Cell Metab* 4:263–273.
- Gimble JM, AJ Katz and BA Bunnell. (2007). Adipose-derived stem cells for regenerative medicine. *Circ Res* 100:1249–1260.
- Bedard K and KH Krause. (2007). The NOX family of ROS-generating NADPH oxidases: physiology and pathophysiology. *Physiol Rev* 87:245.
- Storz P. (2011). Forkhead homeobox type O transcription factors in the responses to oxidative stress. *Antioxid Redox Signal* 14:593–605.
- Finkel T. (2011). Signal transduction by reactive oxygen species. *J Cell Biol* 194:7.
- Loh K, H Deng, A Fukushima, X Cai, B Boivin, S Galic, C Bruce, BJ Shields, B Skiba and LM Ooms. (2009). Reactive oxygen species enhance insulin sensitivity. *Cell Metab* 10:260–272.
- Kim KS, HW Choi, HE Yoon and IY Kim. (2010). Reactive oxygen species generated by NADPH oxidase 2 and 4 are required for chondrogenic differentiation. *J Biol Chem* 285:40294.
- Owusu-Ansah E and U Banerjee. (2009). Reactive oxygen species prime *Drosophila* haematopoietic progenitors for differentiation. *Nature* 461:537–541.
- Furukawa S, T Fujita, M Shimabukuro, M Iwaki, Y Yamada, Y Nakajima, O Nakayama, M Makishima, M Matsuda and I Shimomura. (2004). Increased oxidative stress in obesity and its impact on metabolic syndrome. *J Clin Invest* 114:1752–1761.
- Tormos KV, E Anso, RB Hamanaka, J Eisenbart, J Joseph, B Kalyanaraman and NS Chandel. (2011). Mitochondrial complex III ROS regulate adipocyte differentiation. *Cell Metab* 14:537–544.
- Lee H, YJ Lee, H Choi, EH Ko and J Kim. (2009). Reactive oxygen species facilitate adipocyte differentiation by accelerating mitotic clonal expansion. *J Biol Chem* 284:10601.
- Essers MA, S Weijnen, AM de Vries-Smits, I Saarloos, ND de Ruiten, JL Bos and BM Burgering. (2004). FOXO transcription factor activation by oxidative stress mediated by the small GTPase Ral and JNK. *EMBO J* 23:4802–4812.
- Nakae J, T Kitamura, Y Kitamura, WH Biggs, 3rd, KC Arden and D Accili. (2003). The forkhead transcription factor Foxo1 regulates adipocyte differentiation. *Dev Cell* 4:119–129.
- Munekata K and K Sakamoto. (2009). Forkhead transcription factor Foxo1 is essential for adipocyte differentiation. *In Vitro Cell Dev Biol Anim* 45:642–651.
- Anderson MJ, CS Viars, S Czekay, WK Cavenee and KC Arden. (1998). Cloning and characterization of three human forkhead genes that comprise an FKHR-like gene subfamily. *Genomics* 47:187–199.
- Jacobs FM, LP van der Heide, PJ Wijchers, JP Burbach, MF Hoekman and MP Smidt. (2003). FoxO6, a novel member of the FoxO class of transcription factors with distinct shuttling dynamics. *J Biol Chem* 278:35959–35967.
- Brunet A, A Bonni, MJ Zigmund, MZ Lin, P Juo, LS Hu, MJ Anderson, KC Arden, J Blenis and ME Greenberg. (1999). Akt promotes cell survival by phosphorylating and inhibiting a forkhead transcription factor. *Cell* 96:857–868.
- Tang ED, G Nunez, FG Barr and KL Guan. (1999). Negative regulation of the forkhead transcription factor FKHR by Akt. *J Biol Chem* 274:16741–16746.
- Kojima T, T Norose, K Tsuchiya and K Sakamoto. (2010). Mouse 3T3-L1 cells acquire resistance against oxidative stress as the adipocytes differentiate via the transcription factor FoxO. *Apoptosis* 15:83–93.

26. Calzadilla P, D Sapochnik, S Cosentino, V Diz, L Dicio, JC Calvo and LN Guerra. (2011). N-Acetylcysteine reduces markers of differentiation in 3T3-L1 adipocytes. *Int J Mol Sci* 12:6936–6951.
27. Lin TM, JL Tsai, SD Lin, CS Lai and CC Chang. (2005). Accelerated growth and prolonged lifespan of adipose tissue-derived human mesenchymal stem cells in a medium using reduced calcium and antioxidants. *Stem Cells Dev* 14:92–102.
28. Liu GS, H Peshavariya, M Higuchi, AC Brewer, CW Chang, EC Chan and GJ Dusting. (2012). Microphthalmia-associated transcription factor modulates expression of NADPH oxidase type 4: a negative regulator of melanogenesis. *Free Radic Biol Med* 52:1835–1843.
29. Yoshimura K, T Shigeura, D Matsumoto, T Sato, Y Takaki, E Aiba-Kojima, K Sato, K Inoue, T Nagase, I Koshima and K Gonda. (2006). Characterization of freshly isolated and cultured cells derived from the fatty and fluid portions of liposuction aspirates. *J Cell Physiol* 208:64–76.
30. García-Castro J, C Trigueros, J Madrenas, J Pérez-Simón, R Rodriguez and P Menendez. (2008). Mesenchymal stem cells and their use as cell replacement therapy and disease modelling tool. *J Cell Mol Med* 12:2552–2565.
31. Kanda Y, T Hinata, SW Kang and Y Watanabe. (2011). Reactive oxygen species mediate adipocyte differentiation in mesenchymal stem cells. *Life Sci* 89:250–258.
32. Cheung KJ, I Tzamelis, P Pissios, I Rovira, O Gavrilova, T Ohtsubo, Z Chen, T Finkel, JS Flier and JM Friedman. (2007). Xanthine oxidoreductase is a regulator of adipogenesis and PPAR γ activity. *Cell Metab* 5:115–128.
33. Schroder K, K Wandzioch, I Helmcke and RP Brandes. (2009). Nox4 acts as a switch between differentiation and proliferation in preadipocytes. *Arterioscler Thromb Vasc Biol* 29:239–245.
34. Dansen TB. (2011). Forkhead Box O transcription factors: key players in redox signaling. *Antioxid Redox Signal* 14: 559–561.
35. Laplante M and DM Sabatini. (2009). An emerging role of mTOR in lipid biosynthesis. *Curr Biol* 19:R1046–R1052.
36. Keaney JF, MG Larson, RS Vasan, PWF Wilson, I Lipinska, D Corey, JM Massaro, P Sutherland, JA Vita and EJ Benjamin. (2003). Obesity and systemic oxidative stress. *Arterioscler Thromb Vasc Biol* 23:434–439.
37. Kops GJ, TB Dansen, PE Polderman, I Saarloos, KW Wirtz, PJ Coffey, TT Huang, JL Bos, RH Medema and BM Burgering. (2002). Forkhead transcription factor FOXO3a protects quiescent cells from oxidative stress. *Nature* 419: 316–321.
38. Tothova Z, R Kollipara, BJ Huntly, BH Lee, DH Castrillon, DE Cullen, EP McDowell, S Lazo-Kallanian, IR Williams, et al. (2007). FoxOs are critical mediators of hematopoietic stem cell resistance to physiologic oxidative stress. *Cell* 128:325–339.
39. Tomlinson JJ, A Boudreau, D Wu, H Abdou Salem, A Carrigan, A Gagnon, AJ Mears, A Sorisky, E Atlas and RJ Hache. (2010). Insulin sensitization of human preadipocytes through glucocorticoid hormone induction of forkhead transcription factors. *Mol Endocrinol* 24:104–113.

Address correspondence to:

Dr. Guei-Sheung Liu
Centre for Eye Research Australia
1/32 Gisborne Street
East Melbourne
Victoria 3002
Australia

E-mail: guei-sheung.liu@unimelb.edu.au

Received for publication June 6, 2012

Accepted after revision September 26, 2012

Prepublished on Liebert Instant Online October 1, 2012